DOI 10.1038/s41427-018-0014-9

NPG Asia Materials

ARTICLE Open Access

# High-performance, polymer-based direct cellular interfaces for electrical stimulation and recording

Seong-Min Kim[1], Nara Kim[1,2], Youngseok Kim[1,5], Min-Seo Baik[1], Minsu Yoo[3], Dongyoon Kim[1], Won-June Lee[1], Dong-Hee Kang[1], Sohee Kim[4], Kwanghee Lee[1,2] and Myung-Han Yoon[1]

**Abstract**

Due to the trade-off between their electrical/electrochemical performance and underwater stability, realizing polymer-based, high-performance direct cellular interfaces for electrical stimulation and recording has been very challenging. Herein, we developed transparent and conductive direct cellular interfaces based on a water-stable, high-performance poly(3,4-ethylenedioxythiophene):polystyrene sulfonate (PEDOT:PSS) film via solvent-assisted crystallization. The crystallized PEDOT:PSS on a polyethylene terephthalate (PET) substrate exhibited excellent electrical/electrochemical/optical characteristics, long-term underwater stability without film dissolution/delamination, and good viability for primarily cultured cardiomyocytes and neurons over several weeks. Furthermore, the highly crystallized, nanofibrillar PEDOT:PSS networks enabled dramatically enlarged surface areas and electrochemical activities, which were successfully employed to modulate cardiomyocyte beating via direct electrical stimulation. Finally, the high-performance PEDOT:PSS layer was seamlessly incorporated into transparent microelectrode arrays for efficient, real-time recording of cardiomyocyte action potentials with a high signal fidelity. All these results demonstrate the strong potential of crystallized PEDOT:PSS as a crucial component for a variety of versatile bioelectronic interfaces.

## Introduction

Bioelectronic interfaces that employ diverse conductive matter to electrically interface with biological organs and tissues have been widely utilized to record various bioelectric signals, e.g., brainwaves[1,2], heart beats[3,4] and neuronal spikes[5]. In the case of cellular-level bioelectronic interfaces, direct electrical stimulation has already shown the feasibility of effectively modulating cell body migration[6,7] and neuronal outgrowth[8–10]. In parallel, it has been demonstrated that specific types of cell cultures in contact with conductive materials can induce remarkable phenomena, such as prominent cardiomyocyte activities[11], selective differentiation of neural stem cells into neurons[12], and reduced neuroglial responses[13], even without intentional electrical stimuli. Among a variety of conductive materials, conjugated polymers have attracted researchers owing to their unique properties in conjunction with their decent electrical conductivity, electrochemical activity, optical transparency, and mechanical flexibility, which are highly beneficial for electrically monitoring and stimulating cellular activities in physiological relevant conditions, i.e., aqueous solutions with many ions and biomolecules[14]. Indeed, many research groups have reported various polymer-based bioelectronic interfaces. For instance, polypyrrole[15,16], polyaniline[17,18] and polythiophene[19–21] have been successfully utilized to enhance the sensitivity of biochemical and cellular activity

Correspondence: Kwanghee Lee (klee@gist.ac.kr) or M-H. Yoon (mhyoon@gist.ac.kr)
[1]School of Materials Science and Engineering, Gwangju Institute of Science and Technology, 123 Cheomdan-gwagiro, Buk-gu, Gwangju 61005, Republic of Korea
[2]Heeger Center for Advanced Materials and Research Institute for Solar and Sustainable Energies, Gwangju Institute of Science and Technology, 123 Cheomdan-gwagiro, Buk-gu, Gwangju 61005, Republic of Korea
Full list of author information is available at the end of the article
These authors contributed equally: Seong-Min Kim, Nara Kim.

detection, reduce the threshold potential for neural tissue stimulation, and adjust cellular physiological responses. Thus far, electrochemical polymerization has been mostly employed to fabricate water-stable conjugated polymer films for these purposes[22]. However, current-driving electrodes with a relatively low electrical conductivity, poor surface uniformity, and limited scalability for large-area deposition have been recognized as hurdles in developing more sophisticated, high-performance bioelectronic devices via electropolymerization.

Alternatively, chemically synthesized conjugated polymers have also been utilized for realizing various types of bioelectronic interfaces via solution processing. In particular, poly(3,4-ethylenedioxythiophene):polystyrene sulfonate (PEDOT:PSS) has drawn considerable attention due to its excellent electrical conductivity (>$10^3$ S $cm^{-1}$), high optical transparency (>90%), and low environmental sensitivity in its oxidized/doped form[23,24]. Recently, Malliaras and coworkers discovered that PEDOT:PSS films exhibit a remarkable electrochemical characteristic or "volumetric capacitance", which indicates that its total electrolyte-mediated electrochemical capacitance is proportional to the film thickness, i.e., the volume of a fixed area[25]. In other words, solution-processed PEDOT:PSS films can be applied to high-performance bioelectronic interfaces that require an enhanced electrochemical capacitance to minimize the impedance by increasing the active layer thickness since the total electrochemical capacitance is not necessarily limited by the nominal surface area. However, a serious issue exists in pristine PEDOT:PSS films. An aqueous solution of PEDOT:PSS contains homogeneous, colloidal particles composed of hydrophobic, PEDOT-rich cores and hydrophilic, PSS-rich shells[26,27], which facilitate the deposition of very smooth conductive films with a well-controlled film thickness from aqueous solutions. However, the as-spun PEDOT:PSS film is prone to dissolution or delamination upon water immersion due to an excessive number of water-soluble PSS chains still remaining in the film[28,29]. Although secondary doping or high-temperature thermal treatments of PEDOT:PSS films may improve their mechanical stability in water[30,31], these films swell during prolonged exposure to water due to the hygroscopic nature of the PSS moiety. Therefore, organosilane-based chemical cross-linkers have been introduced into aqueous solutions of PEDOT:PSS along with the surfactant to improve the film durability in water[32,33]. However, cross-linking PEDOT:PSS is not a sufficient remedy to prevent PSS from dissolving in water, and the PSS residues can cause cellular toxicity on direct cellular interfaces. However, a minimalist approach without chemical cross-linkers and/or surfactants to achieve an extraordinary electrical/electrochemical performance in combination with the excellent biocompatibility of solution-deposited PEDOT:PSS films with long-term electrical and mechanical stabilities has not been reported. More importantly, most PEDOT:PSS-based bioelectronics research has been dominated by bioelectric signal recording, and relatively few reports exist on bioelectronic stimulation despite its priority in the therapeutics and treatments of realistic biomedical applications.

Herein, we report PEDOT:PSS-based, highly efficient bioelectronic interfaces with excellent electrical/electrochemical characteristics, long-term underwater stability, and good biocompatibility for direct electrical stimulation and recording of cellular activities. To achieve these goals, highly crystallized PEDOT:PSS (c-PEDOT:PSS) was implemented on plastic substrates (PET) and transparent microelectrode arrays (MEAs). Its electrical performance and long-term stability in an aqueous environment were verified by measuring the electrical conductivity, transparency, and film thickness over time. In parallel, its robustness and excellent electrochemical properties were experimentally verified by comprehensive film analyses. Furthermore, the biocompatibility of c-PEDOT:PSS without chemical cross-linkers and surfactants was evaluated by performing cell viability tests of dividing cell (i.e., NIH-3T3) and primary cell cultures (i.e., neonatal cardiomyocytes) on the film. Finally, the high-performance direct cellular bioelectronic interfaces were successfully demonstrated by effectively modulating the synchronized beating frequency of cardiomyocytes cultured on c-PEDOT:PSS-PET substrates via electrical stimulation and recording the cardiomyocyte action potentials and $Ca^{2+}$ dye fluorescence signals using transparent, high-fidelity MEAs based on c-PEDOT:PSS and Indium Tin Oxide (ITO) layers.

## Materials and methods

### Preparation of the PEDOT:PSS films

The detailed procedure for preparing the PEDOT:PSS substrates is described in the supporting information.

### Fabrication of the transparent c-PEDOT:PSS-ITO microelectrodes arrays (MEAs)

Indium tin oxide (ITO)-coated glass substrates with a sheet resistance of 10 Ω $sq^{-1}$ (Eagle 2000, Corning) were cleaned sequentially with deionized water (DI) water, acetone, and isopropyl alcohol. To define the align mark and low-resistance connection lines, chromium (5 nm) and gold layers (45 nm) were defined via thermal evaporation and conventional lift-off processes. Then, the underlying ITO layer (150 nm) below the Au/Cr lines was patterned by conventional photolithography in combination with a wet-etching process. To decorate the recording sites with the low-impedance c-PEDOT:PSS layer, c-PEDOT:PSS films were deposited onto the substrates with metal and ITO lines and patterned by conventional

photolithography and oxygen plasma etching. Subsequently, the passivation layer to prevent water penetration was defined on top using a primer (Omnicoat, Microchem) and epoxy-based negative photoresist (SU-8, Microchem). The primer layer above c-PEDOT:PSS was stripped by immersing the resultant substrates in a solution of tetramethylammonium hydroxide (300 MIF, Microchem). Finally, acryl-based, truncated tubes were attached on top of the c-PEDOT:PSS-ITO MEAs using polydimethylsiloxane (PDMS) as a glue to define the cell culture reservoir.

#### Evaluation of the water stability of the PEDOT:PSS films

The water stability of the PEDOT:PSS films was studied by repeating the film characterization after the given substrates were immersed in DI water and phosphate-buffered saline (PBS) under the typical cell culture conditions (37 °C and 5% $CO_2$) for a designated period. The film thickness was measured using a surface profilometer (Surfcorder ET-3000, Kosaka Laboratory). The optical transparency in the visible range (at 550 nm) and absorbance spectra were assessed using a ultraviolet–visible/NIR spectrophotometer (Lambda 750, Perkin-Elmer). The electrical conductivity was calculated from the obtained film thickness and sheet resistance.

#### Characterization of the PEDOT:PSS films

The sheet resistance of the PEDOT:PSS films was measured by a four-point probe method. While a constant current was applied using a Keithley 2400 Source Meter unit, the voltage drop was measured using an HP 34401A multimeter. The surface topography images were obtained using an atomic force microscope (AFM; XE-100, Park Systems) or field emission scanning electron microscope (FE-SEM; 6301 F, JEOL). Transmission electron microscopy images were acquired using a Tecnai G2 F30 S-Twin microscope operated at 300 kV. All electrochemical properties were obtained using potentiostats/galvanostats (PGSTAT304N, Metrohm Autolab) equipped with a conventional three-electrode system composed of working, Ag/AgCl reference, and Pt counter electrodes. Cyclic voltammetry (CV) curves were recorded in the range of −0.3 V to 0.3 V at a scan rate of 0.1 V $s^{-1}$. The electrochemical impedance spectroscopy (EIS) analysis was conducted at $E_{dc} = 0$ V with a single sinusoidal signal of $E_{ac} = 25$ mV, and the Bode plots were recorded over a frequency range between $10^{-1}$ and $10^{5}$Hz. The constituent components for an equivalent circuit were extracted using the built-in Autolab software (Nova 1.9, Metrohm Autolab).

#### Cell culture materials

For the fibroblast cultures, a mixture of Dulbecco's modified Eagle medium (DMEM, Gibco) with 10% (v/v) fetal bovine serum (FBS, Corning) was prepared as a medium, and PBS (Gibco) was employed as the washing medium. In the neonatal rat cardiomyocyte culture, the dissection medium was prepared by supplementing 400 ml of phosphate-buffered saline (PBS, Gibco) with 0.8 g of 2,3-butanedione monoxime (BDM, Sigma Aldrich). Hank's balanced salt solution (HBSS, Sigma-Aldrich) was supplemented with 10-mM 4-(2-hydroxyethyl)piperazine-1-ethanesulfonic acid (HEPES, Sigma-Aldrich), 1× penicillin–streptomycin solution (Pen-Strep, HyClone), and 1 mM sodium pyruvate (Sigma-Aldrich). The isolation medium was prepared by supplementing 400 ml of HBSS solution with 0.8 g of BDM and 20 ml of Trysin/EDTA (Sigma Aldrich). The digestion medium was prepared by supplementing 400 ml of Leibovitz's L-15 (L-15, Corning) with 0.8 g of BDM. The plating medium was prepared by supplementing 260 ml of DMEM with 76 ml of Medium 199 (M199, Corning), 60 ml of FBS and 4 ml of Pen-Strep. The maintenance media was prepared by supplementing 312 ml of DMEM with 48 ml of M199, 16 ml of FBS, 4 ml of Pen-Strep, and 50 µl of AraC (Sigma Aldrich). The 10 µl of collagen was dissolved in 10 ml of DI water before use. In the embryonic rat hippocampal neuron culture, a neurobasal medium (Gibco) was supplemented with 5.0 mM GlutaMAX™ (Gibco) and 1 × B-27® serum-free supplement (Gibco). The plating medium was prepared by mixing the 1× DMEM solution with 0.6 wt% d-(+)-glucose (Sigma-Aldrich), 1 mM sodium pyruvate (Gibco), 1× penicillin-streptomycin, 25 mm sodium bicarbonate (Sigma-Aldrich), and 10 mm HEPES, and the final pH was adjusted to 7.4.

#### Cell culture and viability tests with mouse fibroblasts (NIH-3T3)

To check the cell viability, NIH-3T3 cells were deposited on the c-PEDOT:PSS substrates. It is noteworthy that all the substrates for the fibroblast culture were used without any cell adhesive coatings. At day 1 and 3 after the cell seeding, the viable and dead cells were visualized with calcein AM (Santa Cruz Biotechnology) and ethidium homodimer (EthD-1, Molecular Probes), respectively, and they were optically imaged using an inverted fluorescence microscope (IX-71, Olympus) equipped with a 20× lens. The resultant images were used to calculate the cell viability for each substrate.

#### Primary culture of rat neonatal cardiomyocytes

For the primary cardiomyocyte culture, cardiomyocytes were harvested from neonatal rat pups. After decapitating the pups and opening the chest, the hearts were collected in the dissection medium. The collected hearts were cut into small fragments with a scalpel to facilitate the removal of residual blood from the hearts. Subsequently, the fragments were transferred into the isolation medium

and stored at 5 °C overnight with gentle agitation. Then, the fragments were transferred into 10 ml of the digestion medium supplemented with 10 mg collagenase and 10 mg dispase, and oxygen gas was supplied to the media for 1 min to activate the enzymes. After the tissue fragments were stored at 37 °C for 30 min with gentle agitation, they were mechanically dissociated with a 1 ml pipette. The cell-containing media were filtered with a cell strainer (70 μm, Falcon). The harvested cells were collected by centrifuging the filtered media at 1500 rpm for 1 min and then re-dispersed in the plating media. The cells were seeded on a culture flask to remove other types of cells except the cardiomyocytes. After collecting the supernatant media from the culture flask, the cardiomyocytes were seeded on the collagen-coated substrates. After 4 h, the plating medium was replaced by the maintenance medium. All the substrates were coated with collagen before the culture to facilitate the adhesion of cardiomyocytes with a typical cell morphology and function.

#### Primary culture of rat embryonic hippocampal neurons

For the primary neuronal culture, embryonic hippocampi were harvested from Sprague Dawley rat embryos (E18). After decapitating the rat embryos, the hippocampi were extracted from the brains. The collected hippocampi were treated with the diluted papain solution (20 units $ml^{-1}$ in HBSS) after washing with HBSS and stored at 37 °C for 20 min. The resultant suspension was rinsed with the 10% FBS-containing plating medium to inactivate the papain activity, and then, the medium was gradually replaced by HBSS. The treated hippocampi tissues were dissociated by mechanical trituration. After the cells were dissociated from the hippocampal tissues, the cell density in the suspension was measured using a hemocytometer and adjusted to the intended metric by dilution using a 10% FBS-containing plating medium. The as-prepared hippocampal neurons were plated on the given substrates and incubated for 2 h, and then, the culture medium was changed to the neurobasal medium to provide serum-free conditions.

#### Immunofluorescence imaging

To image the spatial distribution of specific proteins, the cultured cells were fixed with 4% paraformaldehyde (Sigma-Aldrich) and 4% sucrose (Sigma-Aldrich) in PBS for 15 min under ambient conditions. After fixation, the cells were treated with 0.25% Triton X-100 (Sigma-Aldrich) in PBS for 5 min to create permeable membranes and then blocked with 4% bovine serum albumin (BSA, Sigma-Aldrich) for 30 min at 37 °C. Next, these cells were treated with primary antibodies in a 1% BSA solution for 12 h at 4 °C and then secondary antibodies tagged with fluorophores. Rabbit polyclonal MAP-2 (200:1, Santa Cruz Biotechnology) and mouse monoclonal tau antibodies (200:1, Santa Cruz Biotechnology) were used to express the axonal differentiation. Mouse monoclonal synapsin (200:1, Santa Cruz Biotechnology) and goat polyclonal PSD-95 antibodies (200:1, Santa Cruz Biotechnology) were used to express synaptogenesis. Rabbit polyclonal connexin-43 (200:1, Sigma Aldrich) and mouse monoclonal α-actinin antibodies (200:1, Sigma Aldrich) were used to express the gap junctions and sarcomeres in cardiomyocytes. Alexa Fluor 546 goat anti-rabbit (1000:1, Molecular Probes), Alexa Fluor 488 goat anti-mouse (1000:1, Molecular Probes), Alexa Fluor 546 goat anti-mouse (1000:1, Molecular Probes), and Alexa Flour 488 chicken anti-goat (1000:1, Molecular Probes) were applied as secondary antibodies.

#### Electrical modulation of the directly cultured cardiomyocytes

To modulate the cardiomyocytes directly cultured on the c-PEDOT:PSS substrates, the c-PEDOT:PSS film and Ag/AgCl electrode were connected to a DAQ board (NI USB-6353, National Instrument) as the working and counter electrodes, respectively. Rectangular biphasic pulse trains with a controlled pulse duration, amplitude, and interpulse interval were applied using a custom-built LabVIEW program.

#### Cardiomyocyte calcium imaging

For the intracellular calcium imaging, 5 μg of the calcium indicator Oregon Green™ 488 BAPTA-1 (Molecular Probes) was dissolved in 1 ml of the neurobasal medium and permeated into the cultured cardiomyocytes by medium replacement. After 10 min of incubation, the medium was replaced with freshly prepared, pre-warmed (37 °C) neurobasal medium and incubated for 30 min. Next, the culture dish was placed on a pre-warmed, live-cell imaging chamber (Chamlide TC-ST, Live Cell Instrument) supplemented with 5% $CO_2$ under an upright fluorescence microscope (IX71, Olympus), and the time-lapse fluorescence images were acquired using an EMCCD (iXon3 885, Andor) under a xenon lamp.

#### Potential recording of the cardiomyocytes via c-PEDOT:PSS-ITO MEAs

The electrical recording and optical imaging were conducted under an inverted microscope (IX71, Olympus), and the whole system was enclosed by a faraday cage to minimize environmental electric noises. The MEAs were connected to an electrical amplifier (Model 1800, AMSYSTEMS) with a gain of 1000 and a bandpass filter between 1 and 5 kHz. The amplified signals were acquired using a data acquisition instrument (Digidata 1550 digitizer, Axon Instruments) with a sampling rate of 50 kHz. The raw data were filtered with a notch filter to reduce the 60 Hz electrical noise, and repeated

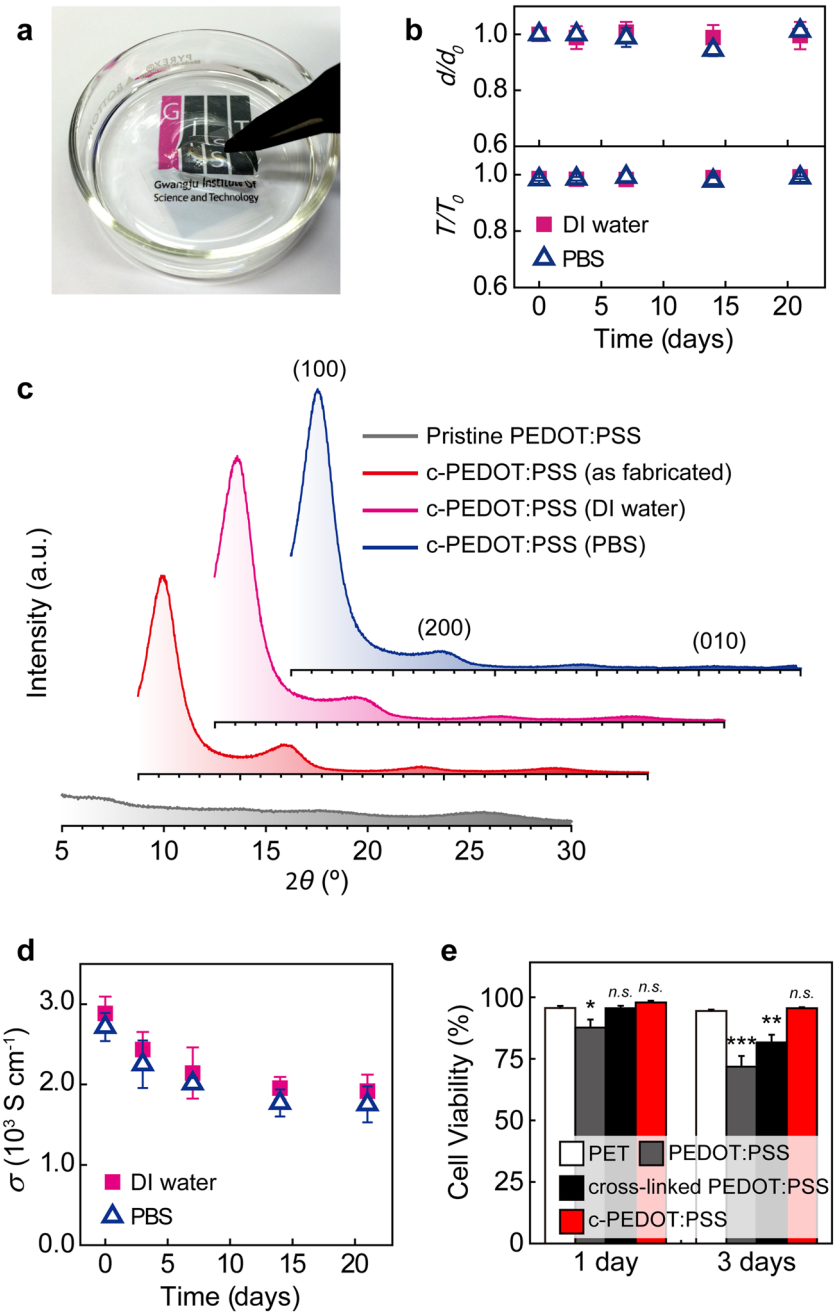


**Fig. 1 c-PEDOT:PSS film characterization. a** A photograph of the c-PEDOT:PSS-PET substrate immersed in water. **b** Plots of the normalized thickness (upper) and optical transmittance of the c-PEDOT:PSS films (lower) with respect to the duration of immersion in DI water and phosphate-buffered saline (PBS). $d_0$ and $T_0$ denote the initial film thickness and transmittance, respectively, at day 0 before water immersion. **c** X-ray diffractograms of pristine PEDOT:PSS and various c-PEDOT:PSS films (as fabricated, immersed in DI water and PBS for 5 days). **d** Plots of the electrical conductivities of c-PEDOT:PSS films with respect to the duration of immersion in DI water and PBS. **e** Statistical distributions of the cell viability on PET, PEDOT:PSS, chemically cross-linked PEDOT:PSS, and c-PEDOT:PSS on PET after 1- and 3-day cultures. NIH-3T3 cells were stained with calcein AM and Hoechst 33342 to identify the viable cells and total cell nuclei, respectively. The data are presented as the mean ± s.e.m., and their variances were evaluated by a two-tailed *t*-test (n.s: not significant, $^{*}P < 0.05$, $^{**}P < 0.01$, $^{***}P < 0.001$, $N = 12$)

spikes were sorted using an embedded tool in the DAQ program (Clampfit, Axon Instrument). To describe the specifications of our MEAs exactly, no filtering processes were conducted.

## Results and discussion

### Film characterization and underwater stability tests

As described in the introduction, the addition of chemical cross-linkers and surfactants to the PEDOT:PSS system causes serious issues, e.g., degradation of the electrical and electrochemical performance and decreased underwater stability and biocompatibility. In this research, we opted for a minimalist approach without additives or residues to achieve the abovementioned goals by crystallizing the PEDOT chains and removing the excess amount of PSS via solvent-assisted crystallization. The fabrication procedure for the c-PEDOT:PSS-PET substrates is illustrated in Figure S1. Briefly, an aqueous solution of PEDOT:PSS (PH1000, Heraeus, USA) was directly spin-coated on a quartz wafer. Subsequently, the as-spun PEDOT:PSS film was immersed into concentrated sulfuric acid for the solvent-assisted crystallization and then thoroughly rinsed with DI water, as described previously[34]. Next, the resulting c-PEDOT:PSS film was transferred onto a PET substrate via a dry transfer using a PDMS stamp[35]. To evaluate the long-term stability in an aqueous environment, the c-PEDOT:PSS-PET substrates were submerged into DI water or phosphate-buffered saline (PBS) during a designated time period, and their thicknesses, optical transmittances, and electrical conductivities were directly compared with those of the pristine PEDOT:PSS-PET substrates; i.e., a PEDOT:PSS solution was directly spin-coated on PET films without chemical cross-linkers. PBS was employed to emulate a physiologically relevant aqueous ionic environment since its pH, osmolality, and ion concentrations match those of human body fluids. Unlike pristine PEDOT:PSS, which immediately dissolved after immersion in DI water (Fig. S2), c-PEDOT:PSS showed excellent adhesion on the flexible PET substrates without film dissolution or delamination (Fig. 1a). The lack of change in the film thickness and adhesion for up to 3 weeks in water can be attributed to the highly ordered structures in PEDOT and the reduced amount of water-wettable PSS in the c-PEDOT:PSS layer (Fig. 1b)[34]. Indeed, as shown in the X-ray diffractograms, distinctive crystalline peaks indicating edge-on lamellar stacking remained in all the c-PEDOT:PSS films regardless of the 5-day DI water or PBS immersion, but the pristine PEDOT:PSS film showed only an amorphous profile (Fig. 1c). It is notable that the Bragg peaks starting at the lowest diffraction angle at $2\theta = 6.2°$ agree with the lattice parameters for PEDOT:PSS lamellar stacking (14.2 Å) with completely alternating edge-on ordering[34,36], and the crystalline signature of the lamellar stacking did not change even after prolonged exposure to DI water or PBS.

Moreover, the bright-field and high-angle annular dark-field scanning transmission electron microscopy as well as AFM topography images indicate that c-PEDOT:PSS consists of highly dense nanofibrillar networks with an enlarged nanoscale porosity and roughness (Fig. S3). Despite a very high initial value (>3000 S $cm^{-1}$), the electrical conductivity of c-PEDOT:PSS gradually decreased and finally stabilized at ~1800 S $cm^{-1}$ after a 10-day immersion in water (Fig. 1d). Nonetheless, this metric is still very high in comparison with the other values reported in the literature[37–39]. Therefore, the robustness of the highly crystalline fibrillar nanostructures is responsible for the long-term electrical, optical, and mechanical stabilities of c-PEDOT:PSS in aqueous, ionic environments[34].

### Dramatic enhancement in the electrochemical activity and biocompatibility

In conjunction with an excellent electrical conductivity and underwater stability, a dramatic enhancement in the electrochemical activity and biocompatibility of the PEDOT:PSS films is crucial for its application in high-performance direct cellular bioelectronic interfaces. Therefore, CV was performed to estimate the electroactive surface areas of both the crystallized and chemically cross-linked PEDOT:PSS films (Fig. S4). The chemically cross-linked PEDOT:PSS was prepared using a mixture of PEDOT:PSS, 20% ethylene glycol, 1% (3-glycidyloxypropyl)trimethoxysilane (GOPS), and 1% dodecyl benzene sulfonic acid (DBSA). This formulation has been widely used for a variety of bioelectronic interfaces reported in previous literature[32,33]. The as-prepared cross-linked PEDOT:PSS films showed a decent electrical conductivity of 263 ± 21 S $cm^{-1}$ at a thickness of 126 nm, and c-PEDOT:PSS films with a similar thickness (~100 nm) were prepared and tested for a direct comparison (Table S1). Remarkably, the c-PEDOT:PSS film exhibited a ~16 times higher current density than the cross-linked PEDOT:PSS film at the same voltage scan rate and range between −0.3 and 0.3 V. In this voltage range, no apparent faradaic reactions were observed on all the PEDOT:PSS films, and the ITO electrode showed a minimal current density (<$10^{-3}$ mA $cm^{-2}$). The much larger current density in c-PEDOT:PSS could be attributed to the substantial increase in the effective surface area and nanoscale porosity (Fig. S3) and the noticeable improvement in both the electrical conductivity and electrochemical capacitance, which was confirmed by the EIS results in the supplementary information (Fig. S5 and Table S2).

In parallel, the cellular toxicity on the c-PEDOT:PSS-PET substrates was investigated by staining live and dead

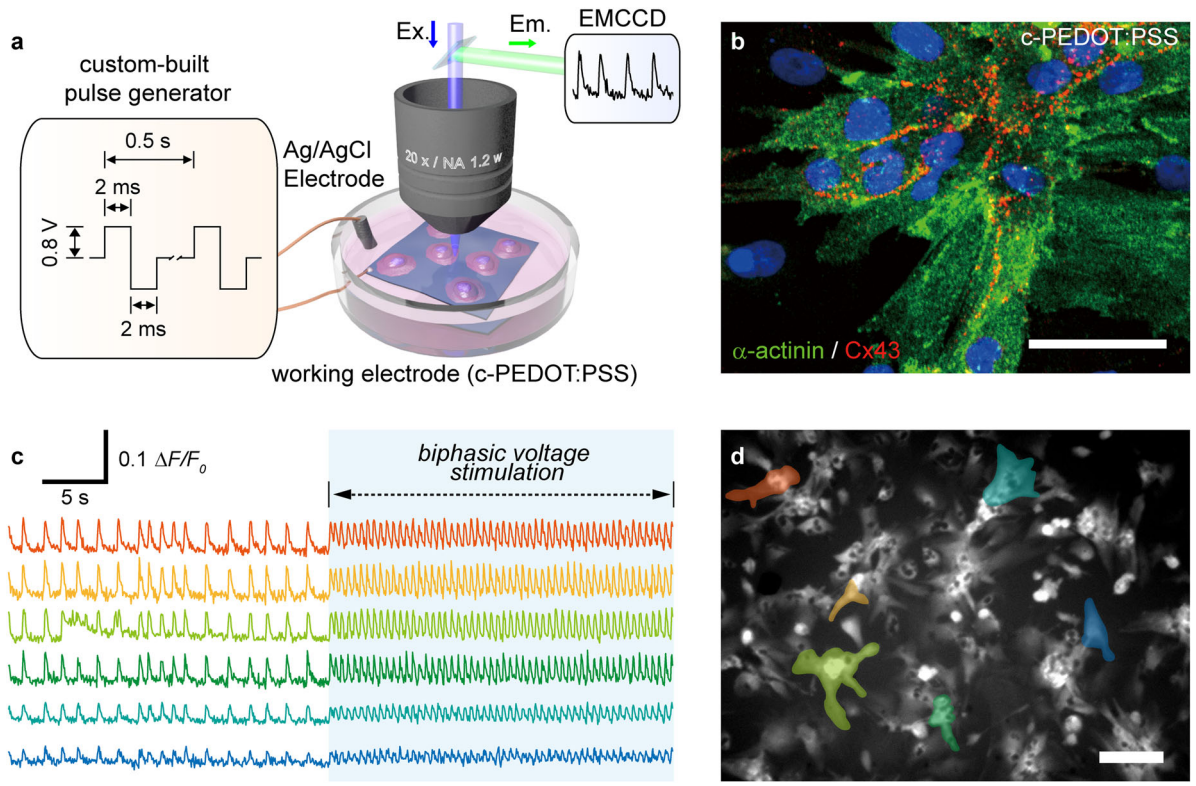


**Fig. 2 The modulation of the beating frequency of cardiomyocytes directly cultured on c-PEDOT:PSS substrates via electrical stimulation.** **a** A schematic of the direct electrical stimulation and optical imaging of the cells. Biphasic voltage pulses were directly applied onto a c-PEDOT:PSS electrode using a custom-built pulse generator, while the intracellular calcium imaging was performed using an EMCCD-equipped upright fluorescence microscope. **b** An immunofluorescence image of neonatal cardiomyocytes (5 DIV) on c-PEDOT:PSS. α-Actinin and connexin 43 are marked with green and red colors, respectively, while the nuclei are identified with DAPI (blue). Both scale bars denote 100 μm. **c** $Ca^{2+}$ signals from the cardiomyocytes on c-PEDOT:PSS before and after electrical stimulation. Each time-lapse $Ca^{2+}$ signal was acquired from the corresponding cell marked with the same color in the optical image. **d** A representative optical image of the cardiomyocytes after electrical stimulation. Viable cells on c-PEDOT:PSS were visualized using calcein AM. The scale bar denotes 100 μm

fibroblast cells (NIH-3T3)[40–42] with calcein AM and ethidium homodimer, respectively. Pre-cleaned PET was used as a control substrate, and cross-linked PEDOT:PSS, and PEDOT:PSS (prepared with an identical recipe used for the cross-linked PEDOT:PSS without cross-linker) were also examined for a direct comparison. As shown in Figure S6, the fibroblasts exhibited good adhesion and normal proliferation on the c-PEDOT:PSS-PET substrates, which was similar to that observed on the control substrates. However, as indicated by the false-colored (red) cells, a considerable number of dead cells were found on both the PEDOT:PSS-PET and cross-linked PEDOT:PSS-PET substrates. Indeed, the cell viability statistics after 1- and 3-day cultures clearly confirmed this trend (Fig. 1e). Both the c-PEDOT:PSS-PET and bare PET substrates support a very high cell viability, over 98%, invariably during the whole culture period. In contrast, both PEDOT:PSS and cross-linked PEDOT:PSS had relatively lower cell viability values, which decreased to 70% for PEDOT:PSS and 82% for cross-linked PEDOT:PSS after 3 days. Considering that the control PET substrate itself is marginally cytotoxic and c-PEDOT:PSS has a much lower amount of residual PSS chains (Fig. S7), the lower cell viability can be attributed to the dissolved PSS chains and residual additives, such as the surfactant (i.e., DBSA) and chemical cross-linker (i.e., GOPS) (Fig. S8), which may cause plasma membrane instability and cellular toxicity[21,43]. Due to the optimal electrical/electrochemical performance and high culture viability, c-PEDOT:PSS was exclusively employed for the long-term primary culture tests and electrical recording/stimulation of cardiomyocyte activities in the following.

### Direct electrical stimulation of cardiomyocytes

Owing to its excellent electrical/electrochemical characteristics, prolonged underwater stability, and cell culture compatibility, we examined the feasibility of direct electric stimulation of electroactive cells using c-PEDOT:PSS as an underwater electrode. Considering that most PEDOT:PSS-based bioelectronic devices have focused on

bioelectric signal recording rather than stimulation, to our knowledge, our work is the first demonstration of a solution-processed PEDOT:PSS for direct cardiac cell stimulation. In this research, cardiomyocytes were selected as a model electrogenic cellular system because it is relatively easy to culture neonatal cardiomyocytes and observe their autonomous synchronized beatings on a laboratory scale. Neonatal rat cardiomyocytes were extracted and cultured directly on top of the c-PEDOT:PSS-PET substrates and stimulated by applying electrical pulses to modulate their synchronized beating frequencies (Fig. 2a). Before the stimulation experiment, the long-term biocompatibility of the primarily cultured neonatal cardiomyocytes was investigated on the c-PEDOT:PSS-PET substrates. When the dissociative culture of the neonatal (P0) myocardium was plated on c-PEDOT:PSS for 5 days in vitro (DIV), good cell viability and reasonably fast maturation was observed and comparable to that observed on the control PET substrates (Fig. 2b and S9). It is noteworthy that the cardiac cells on both c-PEDOT:PSS-PET and the control substrates showed very similar expression patterns of α-actinin and connexin 43, which are responsible for myocardial muscle contractions and gap junction formation, respectively. This result suggests that c-PEDOT:PSS properly supports the viability, maturation, and synchronized beating (*vide infra*) of primarily cultured cardiomyocytes. In addition, we suppose that c-PEDOT:PSS may afford a stable culture environment for a variety of cells subject to "electrical modulation" or direct bioelectronic interfacing with electrophysiologically active cells.

Regarding the electrical stimulation, biphasic voltage pulses were applied using a custom-built LabVIEW program with an amplitude of 0.8 V, duration of 2 ms, and interval of 0.5 s for 1 min (Fig. 2a inset)[44,45], and the intracellular calcium signaling was recorded before and during the stimulation. A low electric potential (<1 V) was employed because a high voltage above 1 V may induce water electrolysis, leading to a pH change in the culture media. Initially, the cultured cardiomyocytes showed synchronized beatings at a relatively slow frequency (0.74 Hz) over the whole substrate. Upon electrical stimulation, their beating frequency immediately increased to ~2 Hz, which well-matched the frequency of the applied pulse

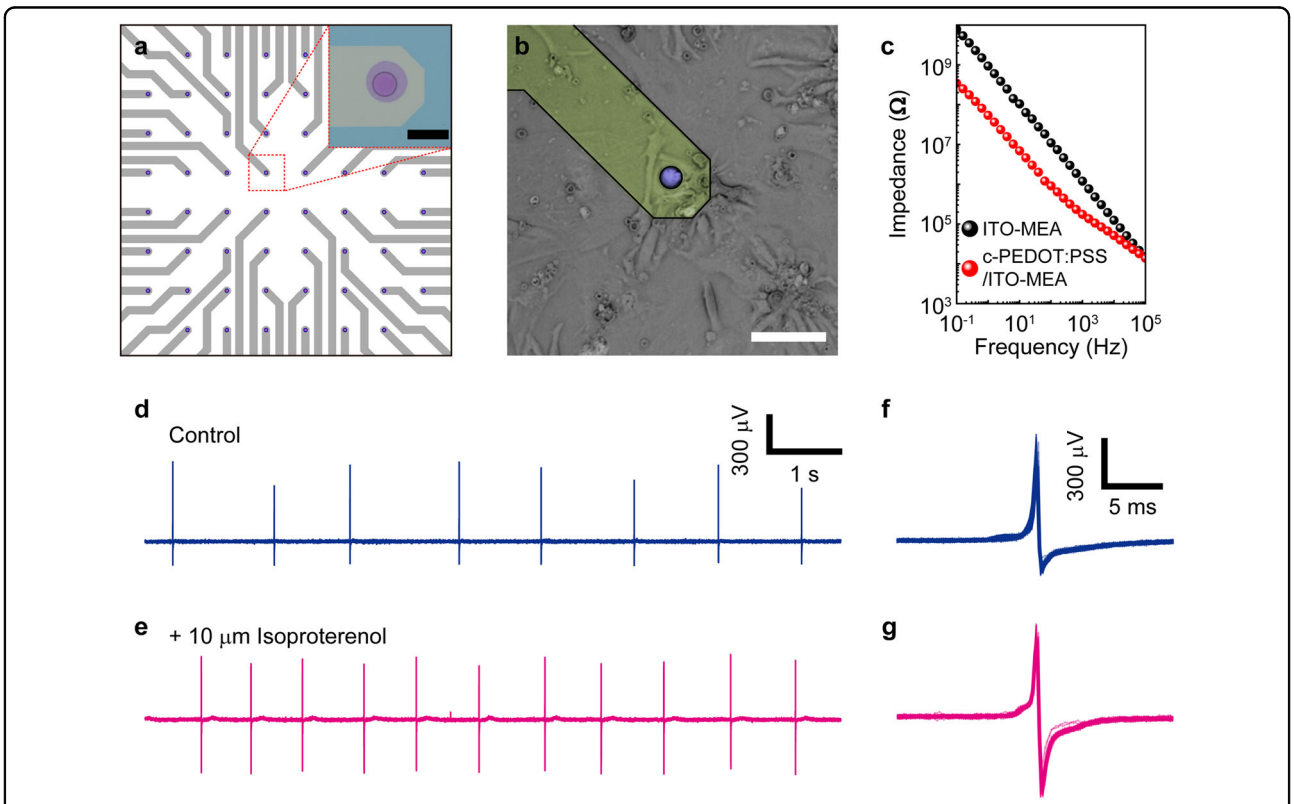


**Fig. 3 Electrical recording of cardiomyocyte activities using c-PEDOT:PSS/ITO-based transparent microelectrode arrays (c-PEDOT:PSS/ITO-MEAs). a** A schematic pattern of a c-PEDOT:PSS/ITO-MEA with an optical micrograph of the recording electrode (inset). The scale bar denotes 50 μm. **b** A phase-contrast image of cardiomyocytes cultured on c-PEDOT:PSS/ITO-MEA. The electrode was false-colored for clarification, and the scale bar denotes 100 μm. **c** Bode plots of impedance on ITO-MEAs and c-PEDOT:PSS/ITO-MEAs. The active electrode exposed to the aqueous electrolyte is a circle with a diameter of 20 μm. **d**, **e** Recorded electrical potential trails of the cardiomyocytes on c-PEDOT:PET/ITO without and with 10 μM isoproterenol added. **f**, **g** Sorted action potentials from **d** and **e**, respectively. ($N = 179$ for control and $N = 91$ for 10 μM isoproterenol)

train (Fig. 2c). Furthermore, most of the cardiomyocytes showed good viability without apparent cell detachment or morphological changes even after long voltage pulse trains for electrical stimulation were directly applied onto the underlying c-PEDOT:PSS-PET substrate (Fig. 2d). These results confirmed that a conductive culture substrate based on c-PEDOT:PSS-PET permits efficient control over the electrophysiological responses of cardiac cells with simple stimulation voltage pulses and favorable culture environments for cellular adhesion and maturation.

### Incorporation into high-performance MEAs and individual cell recordings

The high crystallinity in c-PEDOT:PSS enables its chemical resistance to common organic solvents and various aqueous solutions including cell culture media and water-based developers/etchants. Therefore, the microscale patterning of the c-PEDOT:PSS layer can be easily performed via conventional photolithography and reactive ion etching, and the c-PEDOT:PSS layer was successfully incorporated into ITO-based transparent MEAs (ITO-MEAs, Fig. 3a) with reduced interfacial impedance. It is noteworthy that the optical transparency and high capacitance, i.e., low interfacial impedance of the actual cell contact pad, are essential for high-fidelity electrical recording and concurrent optical imaging (*vide infra*). ITO-MEAs with c-PEDOT:PSS as the active cell contact pads (c-PEDOT:PSS/ITO-MEA) were fabricated as described in the experimental section. The resulting MEAs contain 60 c-PEDOT:PSS recording sites. The concentric circular areas with a diameter of 20 μm are exposed to the aqueous medium or cells, and the entire electrode array, except for the recording sites, was passivated for insulation by an epoxy resist (SU-8). For the stable recording of the cardiomyocyte beatings, the c-PEDOT:PSS/ITO-MEA was installed on a fluorescence microscope inside a faraday cage. Then, cardiomyocytes were directly cultured on c-PEDOT:PSS/ITO-MEA for 5 DIV. As shown in Fig. 3b, cell spreading in the vicinity of a recording electrode was clearly indicated by the phase-contrast microscopy imaging. Noticeably, the c-PEDOT:PSS/ITO-MEAs showed a 10-fold lower impedance than the ITO-MEAs at $10^3$ Hz based on the EIS measurements (Fig. 3c). The c-PEDOT:PSS/ITO-MEAs showed a significantly low impedance and high stability in comparison with those of the crosslinked PEDOT:PSS/ITO-MEAs in all the frequency ranges (data not shown), which implied that the c-PEDOT:PSS/ITO-MEAs are suitable for recording extracellular potentials with a reduced noise level compared with that of bare ITO-based MEAs and crosslinked PEDOT:PSS/ITO-MEAs. Moreover, to verify the ability of c-PEDOT:PSS/ITO-MEAs for real-time extracellular potential measurements, drug testing was conducted by comparing the recorded extracellular action potentials before/after applying 10 μM isoproterenol. This chemical is known to stimulate β1 and β2 adrenergic receptors to increase the beating rate of cardiomyocytes. The actual bioelectric recording was performed for each exposed electrode pad where cardiomyocyte cells were directly plated and cultured. After applying isoproterenol into the culture medium, the effect of the drug was obvious in terms of increasing the beating frequency from 0.78 to 1.18 Hz (Fig. 3d,e) and the signals in the collected action potential plots becoming more negative (Fig. 3f,g).

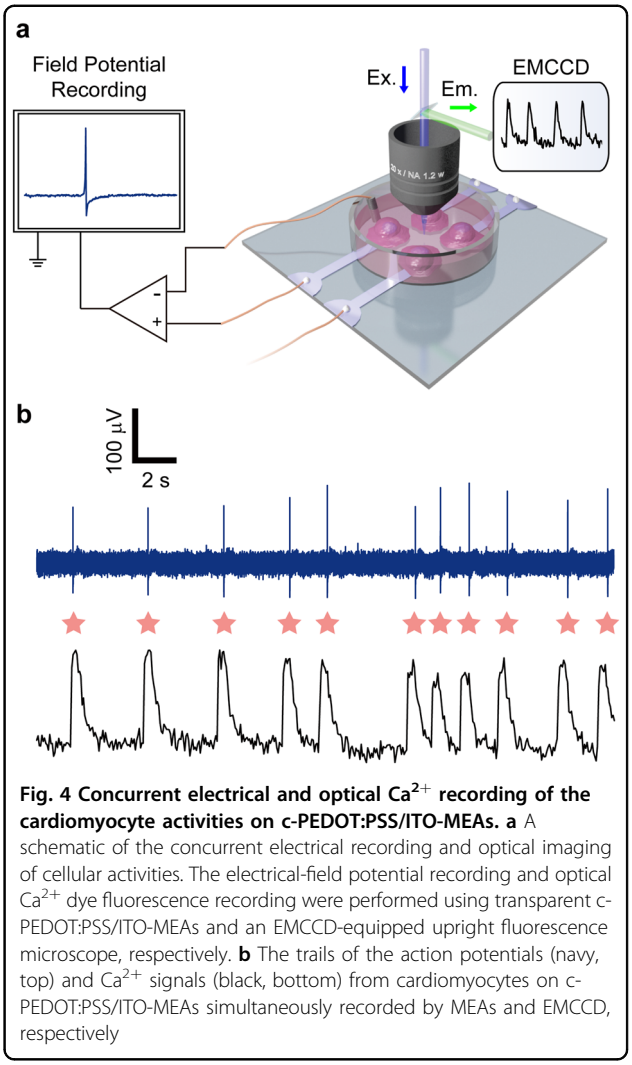


**Fig. 4 Concurrent electrical and optical $Ca^{2+}$ recording of the cardiomyocyte activities on c-PEDOT:PSS/ITO-MEAs. a** A schematic of the concurrent electrical recording and optical imaging of cellular activities. The electrical-field potential recording and optical $Ca^{2+}$ dye fluorescence recording were performed using transparent c-PEDOT:PSS/ITO-MEAs and an EMCCD-equipped upright fluorescence microscope, respectively. **b** The trails of the action potentials (navy, top) and $Ca^{2+}$ signals (black, bottom) from cardiomyocytes on c-PEDOT:PSS/ITO-MEAs simultaneously recorded by MEAs and EMCCD, respectively

### Concurrent recording of bioelectronic and optical $Ca^{2+}$ signals

Finally, concurrent electrical recording and optical calcium imaging were conducted, as depicted in Fig. 4a. Even though the electrical noise from the fluorescence imaging equipment (i.e., EM-CCD) neutralized the high signal-to-noise ratio in the MEA-only recording (see Fig. 3d–g),

Fig. 4 clearly reveals that each recorded action potential spike was temporally synchronized with the corresponding $Ca^{2+}$ signal from the cell(s) near the given recording electrode. In fact, when the action potentials were recorded after disconnecting an electrical noise source (i.e., EM-CCD), the recorded extracellular potential showed a much higher signal-to-noise ratio. All these results indicate that c-PEDOT:PSS is a highly efficient bioelectronic interface for direct electrical stimulation and recording of individual cellular activities.

## Conclusion

In conclusion, we developed high-performance direct cellular interfaces based on water-stable, highly densified nanofibrillar PEDOT:PSS via a solvent-assisted crystallization. The c-PEDOT:PSS exhibited excellent electrical/electrochemical/optical characteristics, long-term underwater stability without film dissolution/delamination, and good viability of primarily cultured cardiomyocytes and neurons. Moreover, the patterning of c-PEDOT:PSS via conventional photolithography and the feasibility of efficient cardiac stimulation and concurrent optical/electrical recordings were experimentally proven. We expect that c-PEDOT:PSS will be beneficial for direct cellular bioelectronic interfaces requiring unprecedented high signal fidelity, operational stability, and biocompatibility, and will lead to the development of a variety of multifunctional, high-performance cell-based biosensors and implantable bioelectronics in the near future.

#### Acknowledgements

This research was supported by the Basic Science Research Program through the National Research Foundation of Korea (NRF) funded by the Ministry of Science and ICT (NRF-2017R1A2B4003873). This research was also supported by the Center for Advanced Soft-Electronics funded by the Ministry of Science, ICT and Future Planning as Global Frontier Project (2013M3A6A5073183), and the GIST Research Institute in 2017.

#### Author details

[1]School of Materials Science and Engineering, Gwangju Institute of Science and Technology, 123 Cheomdan-gwagiro, Buk-gu, Gwangju 61005, Republic of Korea. [2]Heeger Center for Advanced Materials and Research Institute for Solar and Sustainable Energies, Gwangju Institute of Science and Technology, 123 Cheomdan-gwagiro, Buk-gu, Gwangju 61005, Republic of Korea. [3]Department of Neurobiology, University of Chicago, Chicago, IL, USA. [4]Department of Robotics Engineering, Daegu Gyeongbuk Institute of Science and Technology, 333 Techno Jungang Daero, Hyeonpung-Myeon, Dalseong-gun, Daegu 42988, Korea. [5]Present address: Laboratory of Organic Electronics, ITN, Linköping University, SE-601 74 Norrköping, Sweden

#### Author contributions

S.-M.K., N.K., Y.K., K. L. and M.-H.Y. designed all the experiments. S.-M.K., N.K. and Y.K. prepared the PEDOT:PSS films. S.-M.K., N.K., M.-S.B. and W.-J.L. performed the film characterizations. S.-M.K., Y.K., M.-S.B., D.-H.K., M.Y. and D.K. conducted biological experiments. Y.K. fabricated and characterized the multi-electrode arrays (MEAs) and measured the cell potentials using the MEAs. S.-M.K, N.K, Y.K, K. L. and M.-H.Y wrote the manuscript. All authors commented on the manuscript.

#### Conflict of interest

The authors declare that they have no conflict of interest.



**Supplementary information** is available for this paper at https://doi.org/10.1038/s41427-018-0014-9.

Received: 2 October 2017 Revised: 6 December 2017 Accepted: 10 December 2017
Published online: 16 April 2018

#### References

1. Xie, C. et al. Three-dimensional macroporous nanoelectronic networks as minimally invasive brain probes. *Nat. Mater.* **14**, 1286–1292 (2015).
2. Chen, R., Canales, A. & Anikeeva, P. Neural recording and modulation technologies. *Nat. Rev. Mater.* **2**, 16093 (2017).
3. Kim, D.-H. et al. Materials for multifunctional balloon catheters with capabilities in cardiac electrophysiological mapping and ablation therapy. *Nat. Mater.* **10**, 316–323 (2011).
4. Campana, A., Cramer, T., Simon, D. T., Berggren, M. & Biscarini, F. Electrocardiographic recording with conformable organic electrochemical transistor fabricated on resorbable bioscaffold. *Adv. Mater.* **26**, 3874–3878 (2014).
5. Spira, M. E. & Hai, A. Multi-electrode array technologies for neuroscience and cardiology. *Nat. Nanotechnol.* **8**, 83–94 (2013).
6. Yao, L., McCaig, C. D. & Zhao, M. Electrical signals polarize neuronal organelles, direct neuron migration, and orient cell division. *Hippocampus* **19**, 855–868 (2009).
7. Yao, L., Shanley, L., McCaig, C. & Zhao, M. Small applied electric fields guide migration of hippocampal neurons. *J. Cell. Physiol.* **216**, 527–535 (2008).
8. Schmidt, C. E., Shastri, V. R., Vacanti, J. P. & Langer, R. Stimulation of neurite outgrowth using an electrically conducting polymer. *Proc. Natl. Acad. Sci.* **94**, 8948–8953 (1997).
9. Quigley, A. F. et al. A conducting-polymer platform with biodegradable fibers for stimulation and guidance of axonal growth. *Adv. Mater.* **21**, 4393–4397 (2009).
10. Kim, I. et al. Enhanced neurite outgrowth by intracellular stimulation. *Nano Lett.* **15**, 5414–5419 (2015).
11. Mihic, A. et al. A conductive polymer hydrogel supports cell electrical signaling and improves cardiac function after implantation into myocardial infarct. *Circulation* **132**, 772–784 (2015).
12. Park, S. Y. et al. Enhanced differentiation of human neural stem cells into neurons on graphene. *Adv. Mater.* **23**, H263–H267 (2011).
13. Cellot, G. et al. PEDOT:PSS Interfaces support the development of neuronal synaptic networks with reduced neuroglia response in vitro. *Front. Neurosci.* **9**, 521 (2016).
14. Liao, C. et al. Flexible organic electronics in biology: materials and devices. *Adv. Mater.* **27**, 7493–7527 (2014).
15. Geetha, S., Rao, C. R. K., Vijayan, M. & Trivedi, D. C. Biosensing and drug delivery by polypyrrole. *Anal. Chim. Acta* **568**, 119–125 (2006).
16. Cui, X., Wiler, J., Dzaman, M., Altschuler, R. A. & Martin, D. C. In vivo studies of polypyrrole/peptide coated neural probes. *Biomaterials* **24**, 777–787 (2003).
17. Langer, J. J. et al. Polyaniline biosensor for choline determination. *Surf. Sci.* **573**, 140–145 (2004).
18. Wang, L.-P., Wang, W., Di, L., Lu, Y.-N. & Wang, J.-Y. Protein adsorption under electrical stimulation of neural probe coated with polyaniline. *Colloids Surf. B Biointerfaces* **80**, 72–78 (2010).
19. Cui, X. & Martin, D. C. Electrochemical deposition and characterization of poly (3,4-ethylenedioxythiophene) on neural microelectrode arrays. *Sens. Actuators B Chem.* **89**, 92–102 (2003).
20. Ludwig, K. A., Uram, J. D., Yang, J., Martin, D. C. & Kipke, D. R. Chronic neural recordings using silicon microelectrode arrays electrochemically deposited with a poly(3,4-ethylenedioxythiophene) (PEDOT) film. *J. Neural Eng.* **3**, 59 (2006).
21. Berggren, M. & Richter-Dahlfors, A. Organic bioelectronics. *Adv. Mater.* **19**, 3201–3213 (2007).
22. Abidian, M. R. & Martin, D. C. Experimental and theoretical characterization of implantable neural microelectrodes modified with conducting polymer nanotubes. *Biomaterials* **29**, 1273–1283 (2008).

23. Groenendaal, L., Jonas, F., Freitag, D., Pielartzik, H. & Reynolds, J. R. Poly(3,4-ethylenedioxythiophene) and its derivatives: past, present, and future. *Adv. Mater.* **12**, 481–494 (2000).
24. Rivnay, J., Owens, R. M. & Malliaras, G. G. The rise of organic bioelectronics. *Chem. Mater.* **26**, 679–685 (2013).
25. Rivnay, J. et al. High-performance transistors for bioelectronics through tuning of channel thickness. *Sci. Adv* **1**, e1400251–e1400251 (2015).
26. Kirchmeyer, S. & Reuter, K. Scientific importance, properties and growing applications of poly(3,4-ethylenedioxythiophene). *J. Mater. Chem.* **15**, 2077 (2005).
27. Takano, T., Masunaga, H., Fujiwara, A., Okuzaki, H. & Sasaki, T. PEDOT nanocrystal in highly conductive PEDOT:PSS polymer films. *Macromolecules* **45**, 3859–3865 (2012).
28. Vázquez, M., Danielsson, P., Bobacka, J., Lewenstam, A. & Ivaska, A. Solution-cast films of poly(3,4-ethylenedioxythiophene) as ion-to-electron transducers in all-solid-state ion-selective electrodes. *Sens. Actuators B Chem.* **97**, 182–189 (2004).
29. Kumar, P. et al. Effect of channel thickness, electrolyte ions, and dissolved oxygen on the performance of organic electrochemical transistors. *Appl. Phys. Lett.* **107**, 053303 (2015).
30. Greco, F. et al. Ultra-thin conductive free-standing PEDOT/PSS nanofilms. *Soft Matter* **7**, 10642–10650 (2011).
31. Zucca, A. et al. Roll to roll processing of ultraconformable conducting polymer nanosheets. *J. Mater. Chem. C.* **3**, 6539–6548 (2015).
32. Khodagholy, D. et al. Highly conformable conducting polymer electrodes for in vivo recordings. *Adv. Mater.* **23**, H268–H272 (2011).
33. Sessolo, M. et al. Easy-to-fabricate conducting polymer microelectrode arrays. *Adv. Mater.* **25**, 2135–2139 (2013).
34. Kim, N. et al. Highly conductive PEDOT:PSS nanofibrils induced by solution-processed crystallization. *Adv. Mater.* **26**, 2268–2272 (2014).
35. Kim, N. et al. Highly conductive all-plastic electrodes fabricated using a novel chemically controlled transfer-printing method. *Adv. Mater.* **27**, 2317–2323 (2015).
36. Aasmundtveit, K. E. et al. Structure of thin films of poly(3,4-ethylenedioxythiophene). *Synth. Met.* **101**, 561–564 (1999).
37. Kim, Y. H. et al. Highly conductive PEDOT:PSS electrode with optimized solvent and thermal post-treatment for ITO-free organic solar cells. *Adv. Funct. Mater.* **21**, 1076–1081 (2011).
38. Ouyang, J. "Secondary doping" methods to significantly enhance the conductivity of PEDOT:PSS for its application as transparent electrode of optoelectronic devices. *Displays* **34**, 423–436 (2013).
39. Chou, T.-R., Chen, S.-H., Chiang, Y.-T., Lin, Y.-T. & Chao, C.-Y. Highly conductive PEDOT:PSS films by post-treatment with dimethyl sulfoxide for ITO-free liquid crystal display. *J. Mater. Chem. C.* **3**, 3760–3766 (2015).
40. Li, Z. et al. Cellular level biocompatibility and biosafety of ZnO nanowires. *J. Phys. Chem. C.* **112**, 20114–20117 (2008).
41. Luo, S.-C. et al. Poly(3,4-ethylenedioxythiophene) (PEDOT) nanobiointerfaces: thin, ultrasmooth, and functionalized PEDOT Films with in vitro and in vivo biocompatibility. *Langmuir* **24**, 8071–8077 (2008).
42. Ryoo, S.-R., Kim, Y.-K., Kim, M.-H. & Min, D.-H. Behaviors of NIH-3T3 fibroblasts on graphene/carbon nanotubes: proliferation, focal adhesion, and gene transfection studies. *ACS Nano* **4**, 6587–6598 (2010).
43. Dong, L., Joseph, K. L., Witkowski, C. M. & Craig, M. M. Cytotoxicity of single-walled carbon nanotubes suspended in various surfactants. *Nanotechnology* **19**, 255702 (2008).
44. Natarajan, A. et al. Patterned cardiomyocytes on microelectrode arrays as a functional, high information content drug screening platform. *Biomaterials* **32**, 4267–4274 (2011).
45. Abbott, J. et al. CMOS nanoelectrode array for all-electrical intracellular electrophysiological imaging. *Nat. Nanotechnol.* **12**, 460–466 (2017). advance online publication.